



# Substrate specificity of the pyrophosphohydrolase LpxH determines the asymmetry of *Bordetella pertussis* lipid A

Received for publication, July 1, 2018, and in revised form, March 27, 2019. Published, Papers in Press, March 29, 2019. DOI 10.1074/jbc.RA118.004680

✉ Jesús Arenas<sup>†1</sup>, Elder Pupo<sup>§</sup>, ✉ Eline de Jonge<sup>‡</sup>, ✉ Jesús Pérez-Ortega<sup>‡</sup>, Joerg Schaarschmidt<sup>¶</sup>, Peter van der Ley<sup>§</sup>, and Jan Tommassen<sup>‡</sup>

From the <sup>†</sup>Department of Molecular Microbiology and Institute of Biomembranes, Utrecht University, Padualaan 8, 3584 CH Utrecht, The Netherlands, the <sup>§</sup>Institute for Translational Vaccinology (Intravacc), Antonie van Leeuwenhoeklaan 9, 3721 MA Bilthoven, The Netherlands, and the <sup>¶</sup>Computational Structural Biology Group, Bijvoet Center for Biomolecular Research, Utrecht University, Padualaan 8, 3584 CH Utrecht, The Netherlands

Edited by Chris Whitfield

Lipopolysaccharides are anchored to the outer membrane of Gram-negative bacteria by a hydrophobic moiety known as lipid A, which potently activates the host innate immune response. Lipid A of *Bordetella pertussis*, the causative agent of whooping cough, displays unusual structural asymmetry with respect to the length of the acyl chains at the 3 and 3' positions, which are 3OH-C10 and 3OH-C14 chains, respectively. Both chains are attached by the acyltransferase LpxA, the first enzyme in the lipid A biosynthesis pathway, which, in *B. pertussis*, has limited chain length specificity. However, this only partially explains the strict asymmetry of lipid A. In attempts to modulate the endotoxicity of *B. pertussis* lipid A, here we expressed the gene encoding LpxA from *Neisseria meningitidis*, which specifically attaches 3OH-C12 chains, in *B. pertussis*. This expression was lethal, suggesting that one of the downstream enzymes in the lipid A biosynthesis pathway in *B. pertussis* cannot handle precursors with a 3OH-C12 chain. We considered that the UDP-diacylglucosamine pyrophosphohydrolase LpxH could be responsible for this defect as well as for the asymmetry of *B. pertussis* lipid A. Expression of meningococcal LpxH in *B. pertussis* indeed resulted in new symmetric lipid A species with 3OH-C10 or 3OH-C14 chains at both the 3 and 3' positions, as revealed by MS analysis. Furthermore, co-expression of meningococcal *lpxH* and *lpxA* resulted in viable cells that incorporated 3OH-C12 chains in *B. pertussis* lipid A. We conclude that the asymmetry of *B. pertussis* lipid A is determined by the acyl chain length specificity of LpxH.

The outer membrane of Gram-negative bacteria is an asymmetrical bilayer consisting of phospholipids and lipopolysaccharides (LPS)<sup>2</sup> in the inner and outer leaflets, respectively. It

functions as a permeability barrier for harmful compounds from the environment. LPS is responsible for the barrier function of the membrane. It consists of three moieties: lipid A, which anchors LPS in the membrane; a core oligosaccharide; and a long polysaccharide consisting of repeating units, known as the O antigen. This O antigen, however, is lacking in many bacteria, including *Bordetella pertussis*.

Lipid A, also known as endotoxin, is an important signaling molecule for the innate immune system that is recognized by Toll-like receptor 4 (TLR4) and the co-receptor MD-2. Its structure and biosynthesis pathway are generally well conserved among Gram-negative bacteria (1). In *Escherichia coli*, it consists of a glucosamine disaccharide, phosphorylated at the 1 and 4' positions, and 3-hydroxy (3OH) acyl chains linked via amide bonds at the 2 and 2' positions and via ester bonds at the 3 and 3' positions (Fig. 1A). Secondary acyl chains are esterified to the hydroxyl groups of the primary acyl chains at the 2' and 3' positions, generating the characteristic hexa-acylated bis-phosphorylated lipid A of *E. coli*. Lipid A biosynthesis requires nine conserved enzymes (Fig. 2). Biosynthesis is initiated with the transfer of a 3OH-acyl chain from the acyl carrier protein to the 3 position of GlcNAc in the activated sugar UDP-GlcNAc by the acyltransferase LpxA. The resulting product is deacetylated by LpxC and subsequently acylated with a 3OH-acyl chain at the 2 position by LpxD, generating UDP-2,3-diacylglucosamine (UDP-DAG). LpxH then removes a UMP molecule from a portion of the pool of UDP-DAG molecules, generating lipid X, and one lipid X molecule is linked with a UDP-DAG molecule by LpxB. The resulting product is phosphorylated at the 4' position by LpxK, generating lipid IV<sub>A</sub>. After transfer of two 3-deoxy-D-manno-oct-2-ulosonic acid residues to the 6' position by WaaA, the secondary acyl chains are added by the late acyltransferases LpxL and LpxM (1).

Although the biosynthesis route is well conserved, some variation in the lipid A structure is observed between different Gram-negative bacteria. Such variation, which can have profound effects on signaling via the TLR4/MD-2 complex, is in part due to modifications that occur during or after transport of the LPS molecules to the outer membrane and include, among others, acylation, deacylation, and dephosphorylation events (2, 3). Part of the variation, however, is already introduced during the general biosynthesis pathway. For example, comparison of the structures of lipid A from *E. coli* and *Neisseria meningi-*

This work was partially funded by IntraVacc. Part of this work is included in a European Patent Application with reference number 17160604.9.

This article contains Figs. S1–S4, Tables S1–S4, and Results.

<sup>1</sup> To whom correspondence should be addressed: Unit of Microbiology and Immunology, University of Zaragoza, Av. Miguel Servet, 177, 50013 Zaragoza, Spain. Tel.: 34-976762087; E-mail: jaarenas@unizar.es.

<sup>2</sup> The abbreviations used are: LPS, lipopolysaccharide(s); 3OH, 3-hydroxy; UDP-DAG, UDP-2,3-diacylglucosamine; IPTG, isopropyl 1-thio-β-D-galactopyranoside; CID, collision-induced dissociation; ESI, electrospray ionization; BG, Bordet-Gengou; cDNA, complementary DNA; SPE, solid-phase extraction; Tricine, N-[2-hydroxy-1,1-bis(hydroxymethyl)ethyl]glycine; FT, Fourier transform; SEAP, secreted embryonic alkaline phosphatase.

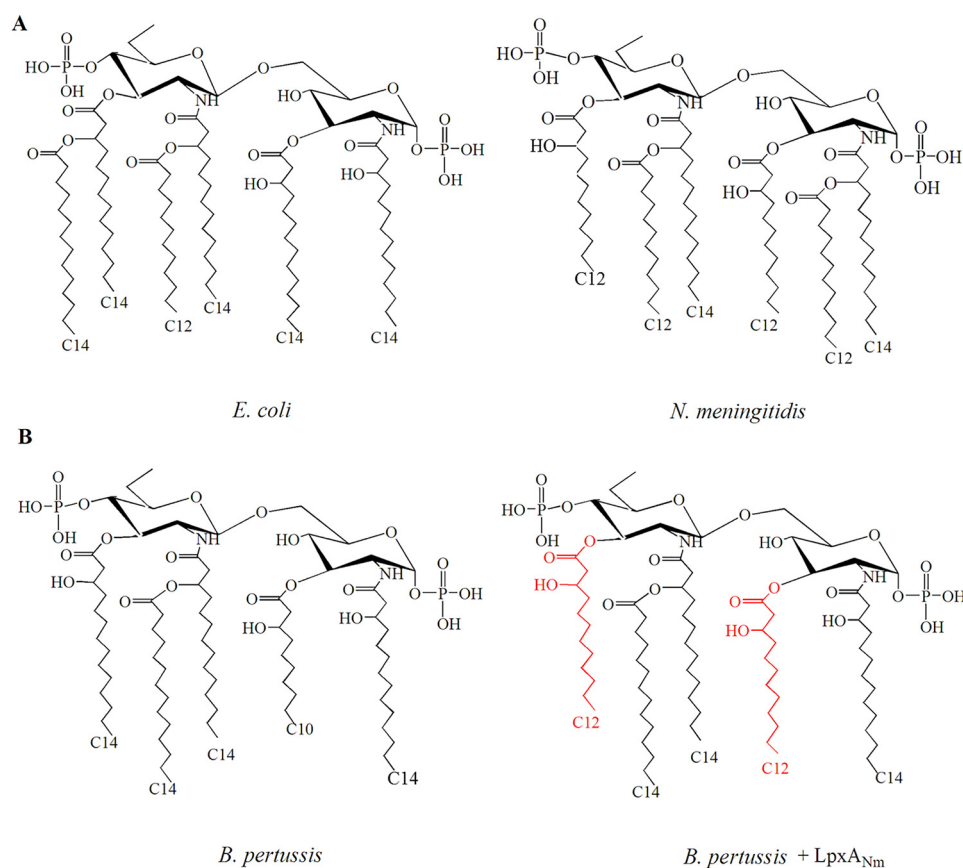


**Figure 1. Lipid A structures.** A, comparison of the structures of lipid A from *E. coli* K-12 and from *N. meningitidis* H44/76. B, structure of lipid A from *B. pertussis* strain B213 and that expected by expression of *lpxA<sub>Nm</sub>* in this strain. The acyl chains that are expected to replace those of the WT in the recombinant strain are indicated in red.

*tidis* shows a different position of one of the secondary acyl chains and a different length of several acyl chains (Fig. 1A). Acyl chain length is determined by hydrocarbon rulers in the acyltransferases (4, 5). Thus, although LpxA of *E. coli* mediates the incorporation of 3OH-C14 chains at the 3 and 3' positions of lipid A, LpxA of *N. meningitidis* (LpxA<sub>Nm</sub>) incorporates 3OH-C12 chains. Because acyl chain length influences the toxicity of lipid A (6, 7), the heterologous expression of acyltransferases can be used in vaccine development projects to modulate lipid A acyl chain length and, thereby, the reactogenicity of vaccine formulations (8).

We are following this approach in the development of a third-generation vaccine against *B. pertussis*, the causative agent of whooping cough. A whole cell-based vaccine against this pathogen, which was introduced in the 1950s, was effective, but it was too reactogenic and therefore replaced with subunit vaccines around the start of the millennium (9). However, these vaccines are insufficiently effective considering the current epidemics of pertussis in industrialized countries where they are implemented, despite high vaccine coverage (10). One approach to solve the problem could be the development of new, less reactogenic cellular vaccines. Because LPS is a major contributor to the toxicity of cellular *B. pertussis* vaccines (11), engineering of the lipid A moiety could offer a solution. *B. pertussis* lipid A has five acyl chains (12). Curiously, the lengths of the acyl chains at the 3 and 3' positions are different (Fig. 1B), even though LpxA is responsible for the incorporation of both

of them. This asymmetry is only partially explained by the relaxed acyl chain specificity of *B. pertussis* LpxA (LpxA<sub>Bp</sub>), which mediates the incorporation of 3OH-acyl chains of various lengths at both the 3 and the 3' position when expressed in *E. coli* (13). In this study, we intended to express LpxA<sub>Nm</sub> in *B. pertussis* to manipulate the reactogenicity of its LPS, but this turned out to be lethal. This observation put us on track to understand the enigmatic asymmetry in *B. pertussis* lipid A with respect to the length of the acyl chains at the 3 and 3' positions.

## Results and discussion

### Heterologous expression of *lpxA<sub>Nm</sub>* in *B. pertussis* is lethal

To modulate LPS toxicity, we intended to express *lpxA<sub>Nm</sub>* in *B. pertussis*, which was expected to result in substitution of the 3OH-C10 and 3OH-C14 acyl chains at the 3 and 3' positions, respectively, of *B. pertussis* lipid A by two 3OH-C12 chains (Fig. 1B). The *lpxA<sub>Nm</sub>* gene was cloned into the broad host range expression vector pMMB67EH under control of the *tac* promoter, and its expression was evaluated in the cloning host *E. coli* BL21(DE3). RT-PCR assays confirmed the presence of transcripts of the *lpxA<sub>Nm</sub>* gene when the bacteria were grown with isopropyl 1-thio- $\beta$ -D-galactopyranoside (IPTG) (Fig. S1A). Expression of *lpxA<sub>Nm</sub>* did not affect the growth of *E. coli*. The plasmid was then transferred by conjugation to *B. pertussis* strain B213. Although some ampicillin- and nalidixic acid-resistant transconjugants were obtained, these colonies failed

## Substrate specificity of *B. pertussis* LpxH

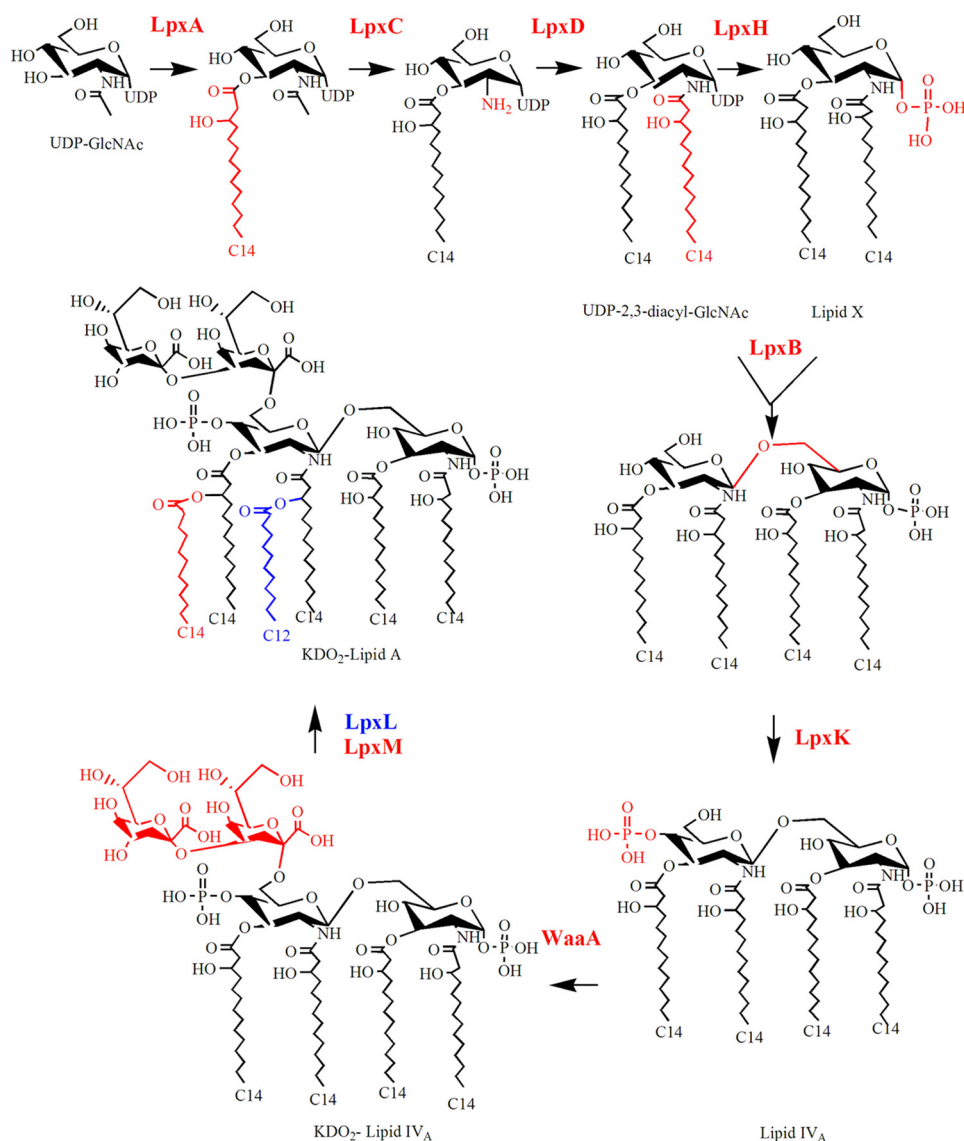


**Figure 2. Schematic representation of the Raetz pathway for the synthesis of Kdo<sub>2</sub>-lipid A.** Shown is the pathway as operative in *E. coli* K-12 according to Ref. 1. The pathway is composed of nine conserved enzymes located in the cytoplasm or the cytoplasmic membrane. The chemical structure of substrates and products of the reactions is indicated. From the top left, arrows show the order of reactions, and the corresponding enzymes are colored according to the resulting structural modification of the product. Where appropriate, the names of substrates or products are specified.

to grow after replating on growth medium containing ampicillin and nalidixic acid. Thus, apparently, even in the absence of IPTG, leaky expression of *lpxA*<sub>Nm</sub> is already lethal in *B. pertussis*, although this is not the case in *E. coli*.

Previously, it has been noticed that incorporation of shorter acyl chains, *i.e.* 3OH-C10 or 3OH-C12, at the 3' position of *B. pertussis* lipid A is possible without affecting viability by a mutation in the endogenous *lpxA*<sub>Bp</sub> gene present in naturally occurring *B. pertussis* isolates (14, 15). Apparently, the problem is that *B. pertussis* cannot incorporate longer acyl chains at the 3 position. Thus, both the lethality of *lpxA*<sub>Nm</sub> expression and the asymmetry of *B. pertussis* lipid A could be explained by assuming that LpxH<sub>Bp</sub>, which releases UMP from a portion of the pool of UDP-DAG molecules (Fig. 2), is highly selective for UDP-DAG molecules that have 3OH-C10 at the 3 position of the sugar moiety. In this way, glucosamine with a 3OH-C10 at the 3 position would always end up at the reducing end of the lipid A disaccharide, whereas the remaining pool of UDP-DAG

molecules with longer acyl chains would end up at the non-reducing end. In addition, when the pool of UDP-DAG molecules with 3OH-C10 is limited because of heterologous expression of an LpxA that only incorporates longer 3OH-acyl chains, such as that of *N. meningitidis*, this would become lethal. An alternative explanation would be that substrate selectivity resides in LpxB<sub>Bp</sub>, which then should selectively incorporate only lipid X molecules with a 3OH-C10 chain at the reducing end in the lipid A precursors (Fig. 2). However, in the absence of LpxH selectivity, numerous lipid X molecules with longer 3OH-acyl chains at the 3 position would be generated, which would be lost for further incorporation into lipid A precursors, which seems highly unlikely.

### Heterologous expression of *lpxH* from *N. meningitidis* (*lpxH*<sub>Nm</sub>) breaks lipid A asymmetry in *B. pertussis*

If our hypothesis that the rigorous asymmetry of lipid A of *B. pertussis* at the 3 and 3' positions is determined by substrate

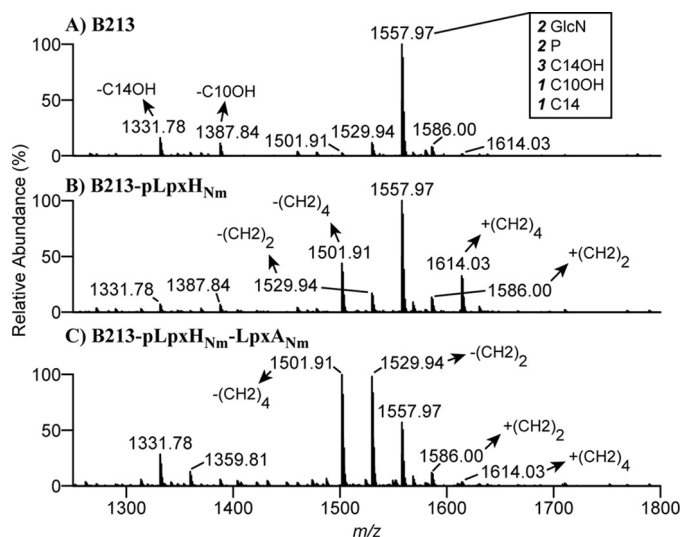


**Figure 3. Structural analysis of lipid A.** A–C, negative-ion lipid A mass spectra were obtained by in-source CID nano-ESI–FT–MS of intact LPS isolated from cells of B213 (A), B213 expressing *lpxH<sub>Nm</sub>* (B), and B213 expressing *lpxH<sub>Nm</sub>* and *lpxA<sub>Nm</sub>* (C). Bacteria were grown for 12 h in Verwey medium in the presence of IPTG. A major singly deprotonated ion at *m/z* 1557.97 was interpreted as the typical *B. pertussis* lipid A structure: a diglucosamine (2 GlcN), penta-acylated (three 3OH-C14, one 3OH-C1, and one C14) with two phosphate residues (2 P), as illustrated in Fig. 1B. Additional singly deprotonated lipid A ions were detected in different derivatives, and their interpretations are indicated. Only the *m/z* range covering lipid A ions is shown.

specificity of LpxH<sub>Bp</sub> is correct, then one would expect that the expression of a heterologous LpxH would break this asymmetry. To test this hypothesis, we cloned the *lpxH<sub>Nm</sub>* gene into plasmid pMMB67EH, whereby a His tag was engineered at the C terminus to facilitate protein detection. Western blotting revealed that the recombinant protein was produced in *E. coli* strain BL21(DE3) even when the strain was grown in the absence of IPTG (Fig. S1B), and no growth defects were observed. The plasmid was then transferred to *B. pertussis* strain B213, where again protein expression was confirmed by Western blotting (Fig. S1B). However, the growth rate of B213 was affected by expression of *lpxH<sub>Nm</sub>* (Fig. S1C). LPS was isolated from the WT strain and from a transconjugant grown in the presence of IPTG. Analysis of the lipid A structure of the WT strain by nano-electrospray ionization (ESI)–MS showed a major peak at *m/z* 1557.97 (Fig. 3A), which corresponds with the expected bis-phosphorylated penta-acylated lipid A (Fig. 1B). The spectrum of B213-pLpxH<sub>Nm</sub> lipid A revealed, besides the ion at *m/z* 1557.97, two additional major ions at *m/z* 1501.91 and *m/z* 1614.03 (Fig. 3B), consistent with the presence of lipid A species with two 3OH-C10 and two 3OH-C14, respectively, at the 3 and 3' positions. These data clearly show that longer acyl chains can be incorporated at the 3 position and shorter acyl chains at the 3' position in *B. pertussis* expressing *lpxH<sub>Nm</sub>* and, thus, that substrate specificity of LpxH<sub>Bp</sub> is responsible for the observed lipid A asymmetry. It should be noted that, because apparently any available acyl chain can be incorporated at the 3 and 3' positions in the recombinant strain, the major ion at *m/z* 1557.97 could consist of two species in this strain, *i.e.* one with 3OH-C10 and 3OH-C14 at the 3 and 3' positions, respectively, like in the WT, and the other having these acyl chains in the reversed positions. Indeed, in-source

collision-induced dissociation (CID) tandem MS (MS/MS) analysis provided evidence of the presence of both species in this ion (see supporting Results).

### Co-expression of *lpxH<sub>Nm</sub>* enables expression of *lpxA<sub>Nm</sub>* in *B. pertussis*

We reasoned that *lpxA<sub>Nm</sub>* expression is lethal in *B. pertussis* because the pool of UDP-DAG molecules with 3OH-C10 chains, which serve as substrates for LpxH<sub>Bp</sub>, is too small in such recombinant strains to generate sufficient lipid X for LPS synthesis. Another explanation could be toxicity of accumulated UDP-DAG molecules with longer acyl chains that cannot be converted by LpxH<sub>Bp</sub>, as reported for an *Acinetobacter baumannii* *lpxH* knockout mutant (15). If either one of these explanations is correct, then co-expression of *lpxH<sub>Nm</sub>* should rescue *B. pertussis* expressing *lpxA<sub>Nm</sub>* because it can also convert UDP-DAG molecules with larger acyl chains at the 3 position into lipid X. To test this possibility, we cloned the *lpxH<sub>Nm</sub>* gene into pMMB67EH-LpxA<sub>Nm</sub> in between the promoter and the *lpxA<sub>Nm</sub>* gene. RT-PCR assays confirmed expression of both genes in *E. coli* (Fig. S1A). The plasmid was then transferred to *B. pertussis* strain B213, and viable transconjugants were obtained, although their growth was reduced compared with WT B213, resulting in about 2-fold lower optical density in the stationary phase (Fig. S1C). This evidences that *lpxH<sub>Nm</sub>* expression can compensate for the lethal effects of the expression of *lpxA<sub>Nm</sub>* in *B. pertussis* and supports the hypothesis that substrate specificity of LpxH<sub>Bp</sub> is responsible for the impaired growth of *B. pertussis* expressing *lpxA<sub>Nm</sub>*. The nano-ESI–MS spectra of lipid A from the recombinant strain showed, besides a large alteration in the relative abundance of the ions at *m/z* 1557.97 and 1501.91, a new major ion at *m/z* 1529.94 (Fig. 3C), which corresponds with lipid A species with 3OH-C10 and 3OH-C12 chains at the 3 and 3' positions, respectively, or in the reversed positions, as evidenced by CID-MS/MS (see expanded results in supporting information file 2). Thus, the 3OH-C12 chains that are introduced in the lipid A biosynthesis pathway by the heterologous LpxA<sub>Nm</sub> end up in the final product. It should be noted that the ion at *m/z* 1557.97 in this case could consist of three lipid A species, *i.e.* the WT with 3OH-C14 and 3OH-C10 at the 3' and 3 positions, respectively, a variant with these chains in the reversed positions, and one with 3OH-C12 at both positions. CID-MS/MS indeed provided evidence for the presence of all three variants in this ion (supporting Results).

### Structural analysis of substrate selection by LpxH

Recently, the crystal structures of LpxH from *Haemophilus influenzae* and from *Pseudomonas aeruginosa* were both solved in complex with the lipid X product of the enzyme (16, 17). LpxH consists of two domains: a catalytic domain homologous to metallophosphoesterases and a helical insertion domain, dubbed the lid, inserted in the middle of the catalytic domain. The catalytic domain of ~180 residues is composed of two facing  $\beta$  sheets and four peripheral  $\alpha$  helices. The lid is composed of two long helices (helix  $\alpha$ 1' and helix  $\alpha$ 3') connected by a short helix (helix  $\alpha$ 2') (Fig. S2). Lipid X locates in the crevice between these two domains, with its phosphate group facing

## Substrate specificity of *B. pertussis* LpxH

the dinuclear metal ( $Mn^{+2}$ ) center and the 2-*N*-linked acyl chain buried in the hydrophobic cavity between the catalytic domain and the lid, whereas the 3-*O*-linked chain reaches out of this cavity and is associated with the surface of the lid. Alignments showed differences in LpxH of *B. pertussis* in this lid domain (Fig. S2A). Structural modeling yielded reasonable models of *B. pertussis* LpxH in complex with lipid X with either 3OH-C14 or 3OH-C10 chains at the 3 position (Fig. S2B). Despite variations in the amino acid composition at the interface with the acyl chain (Fig. S2C), no discernable difference in conformational binding (Fig. S2B) or binding affinity of the two lipid X species were observed (the average Haddock score for 3OH-C10 and 3OH-C14 chains were  $-112 \pm 1.1$  and  $-115.5 \pm 2.8$ , respectively). Notably, the terminal part of the 3OH acyl chain in one of the template structures also protrudes from the complex, suggesting that there are no relevant specific interactions with LpxH in the bound complex whose alteration could promote selectivity. Thus, selectivity is most likely a result of changes in binding kinetics not captured in our model. Based on the suggested binding mode (16), the 3OH acyl chain has to pass through the lid domain upon ligand binding. It is thus possible that specificity is mediated by structural differences in the lid domain of *B. pertussis*, e.g. the differences in the connection loops to helix  $\alpha 2'$  that hinder passage of acyl chains exceeding C10. Possibly, molecular dynamics can give more insight into the specific mechanism.

### Consequence of breaking lipid A asymmetry on membrane permeability

LPS is crucial for the permeability barrier imposed by the outer membrane. To test the biological consequences of changing LpxH specificity, we incubated *B. pertussis* and derivatives with a set of antibiotics (rifampicin, chloramphenicol, and vancomycin) and determined bacterial survival. Rifampicin is a large hydrophobic antibiotic that crosses the outer membrane by diffusion via the hydrophobic pathway. In contrast, chloramphenicol and vancomycin are hydrophilic. Although chloramphenicol can cross the outer membrane by diffusion through the porins, vancomycin is too large and requires membrane disruptions to pass. WT B213 cells were significantly more susceptible to rifampicin than its derivatives expressing *lpxH<sub>Nm</sub>* alone or in combination with *lpxA<sub>Nm</sub>* (Fig. 4). This result indicates that the permeability barrier for hydrophobic compounds imposed by the outer membrane is fortified by expression of the heterologous *lpxH*, although we cannot rule out the possibility that the reduced growth rate of the recombinant strains influences their rifampicin susceptibility. In contrast, expression of *lpxH<sub>Nm</sub>* did not affect the strains' susceptibility to vancomycin and chloramphenicol (Fig. 4), indicating that no breaches were generated in the outer membrane and that the porin pathway for the uptake of hydrophilic compounds was unaffected. The strain expressing both *lpxH<sub>Nm</sub>* and *lpxA<sub>Nm</sub>* was significantly more susceptible to chloramphenicol and also appeared to be somewhat more susceptible to vancomycin, but not significantly (Fig. 4). We also tested the susceptibility of the bacteria to another large hydrophilic antibiotic, bacitracin, but all strains were resistant to the highest concentration tested ( $0.1 \text{ mg ml}^{-1}$ ).

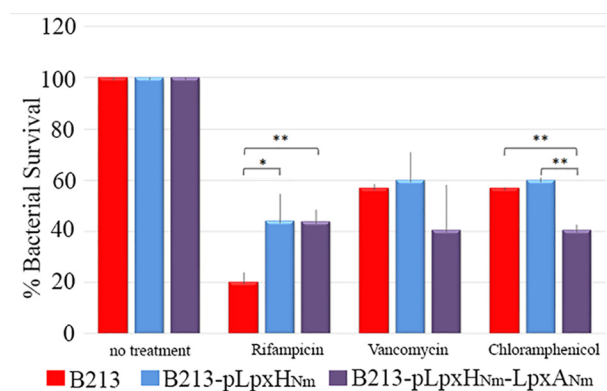


**Figure 4. Antibiotic sensitivity assays.** Bacteria were grown in Verwey medium in the presence of IPTG until the exponential phase and incubated with rifampicin, chloramphenicol, or vancomycin for 1 h. Subsequently, they were plated on BG blood plates, and colonies were counted after 48 h. Bacterial survival is expressed as the percentage of bacteria relative to the untreated control for each strain, and standard deviations are depicted. Data represent results of at least three independent experiments. Statistically significant differences were analyzed with GraphPad Prism 6 (unpaired statistical *t* test). \*,  $p < 0.05$ ; \*\*,  $p < 0.01$ .

### Consequence of breaking lipid A asymmetry on bioactivity

We also analyzed the consequences of LpxH<sub>Nm</sub> activity in *B. pertussis* on TLR4 activation. When HEK-Blue reporter cells expressing the human TLR4 receptor (hTLR4) or mouse TLR4 receptor (mTLR4) were incubated with *B. pertussis* LPS, LPS from strain B213-pLpxH<sub>Nm</sub> showed a similar activation of both hTLR4 and mTLR4 as WT LPS (Figs. 5, A and B). It should be noted, however, that lipid A in the recombinant strain is heterogeneous (Fig. 3B). Hence, even if the bioactivity of some LPS molecules may be changed relative to WT LPS, this is then apparently compensated by altered bioactivity of other LPS molecules in the recombinant cells.

Interestingly, the biological activity of LPS from B213-pLpxH<sub>Nm</sub>-LpxA<sub>Nm</sub> was impaired in the activation of hTLR4 and also, but to lesser extent, of mTLR4 (Fig. 5, A and B), possibly as consequence of the novel lipid A species with 3OH-C12 at the 3 and/or 3' positions produced by this mutant. The lack of hTLR4 activation, despite the presence of also WT LPS in this preparation, indicates that the novel species may have antagonist activity. Thus, these data suggest that alteration of the length of the acyl chains affects the activity of *B. pertussis* LPS, which is consistent with previously described data obtained with natural *B. pertussis* variants producing LPS with a shorter acyl chain at the 3' position (14).

### Conclusion

We have shown, for the first time, that the acyl chain length in lipid A molecules is not only determined by the substrate specificity of the acyltransferases but can also be influenced by substrate specificity of other enzymes in the lipid A biosynthesis pathway, i.e. LpxH. Asymmetric lipid A species, with respect to acyl chain length, are also reported for other bacteria, e.g. in *Piscirickettsia salmonis*, where the major lipid A species contains 3OH-C14 and 3OH-C16 chains at the 2' and 2 positions, respectively (18). However, a minor, symmetric lipid A species was also detected in this species, with 3OH-C14 at both positions. These structures could be explained by a preference but

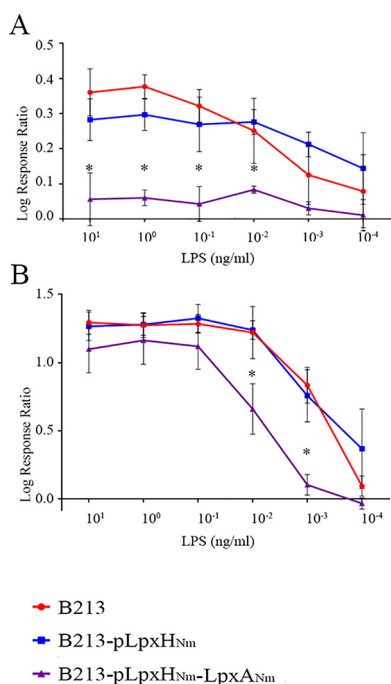


**Figure 5.** A and B, stimulation of HEK293-Blue reporter cells expressing hTLR4 (A) or mTLR4 (B) with purified LPS of strain B213 or mutant derivatives. After incubation of HEK293-Blue cells with the indicated LPS variants for 17 h, alkaline phosphatase activity was determined. Graphs show the log response ratio from three independent experiments with average and standard deviation (error bars). Statistically significant differences were analyzed with GraphPad Prism 6. \*,  $p < 0.05$ .

no strict specificity of LpxH for UDP-DAG molecules with 3OH-C16 at the 2 position in this organism. As another example, *Francisella novicida* produces two LpxD enzymes, one incorporating 3OH-C18 at 37 °C and the other incorporating 3OH-C16 at 18 °C, resulting in symmetric lipid A species at both temperatures (19). However, at intermediate temperature (25 °C), asymmetric lipid A species are produced with 3OH-C18 and 3OH-C16 at the 3' and 3 positions, respectively. This could be explained by a preference, but no strict specificity, of LpxH for UDP-DAG molecules with 3OH-C16 at the 2 position. The knowledge that LpxH can display chain length preference or specificity introduces a new tool that can be used to modulate the composition and, therefore, the reactogenicity of lipid A.

## Experimental procedures

### Plasmids, strains, and growth conditions

The plasmids and strains used in this study are listed in Table S1. *B. pertussis* strains were cultured on Bordet–Gengou (BG) agar (Difco) supplemented with 15% defibrinated sheep blood (Biotrading) for 48 h at 35 °C. To grow the bacteria in liquid cultures, bacteria were collected from BG medium and diluted in Verwey medium (20) to an  $A_{590}$  of 0.05 and incubated with constant shaking at 175 rpm. After growth, bacteria were heat-inactivated for 1 h at 60 °C, harvested by centrifugation at  $3500 \times g$  for 10 min, and stored at -20 °C. *E. coli* strains were grown in lysogeny broth or lysogeny broth agar at 37 °C. For all strains, media were supplemented with ampicillin (100  $\mu\text{g ml}^{-1}$ ) and/or nalidixic acid (50  $\mu\text{g ml}^{-1}$ ) when required for selection and with 0.1 or 1 mM IPTG for *E. coli* or *B. pertussis*, respectively, to induce gene expression.

### Genetic manipulations

Genomic DNA was obtained by resuspending bacteria in water to an  $A_{550}$  of ~2.0. After boiling for 5 min, the cell debris was pelleted in an Eppendorf 5424 centrifuge for 10 min at maximal speed. The supernatant was used as template DNA for PCRs. Primers are listed in Table S2. PCRs were performed using High Fidelity Polymerase (Roche Diagnostics GmbH). PCR mixtures consisted of 1  $\mu\text{l}$  of template DNA, 200  $\mu\text{M}$  dNTPs (Fermentas), 0.25  $\mu\text{M}$  of different primer combinations, 0.5 units of DNA polymerase, and PCR buffer. PCR mixtures were incubated in a thermocycler for 10 min at 95 °C for DNA denaturation, followed by 30 cycles of 1 min at 95 °C, 0.5 min at 58 °C, and elongation at 72 °C for 1 min per kb of the expected amplicon size. The PCRs were finalized by an elongation step for 10 min at 72 °C. The PCR products were analyzed on 1% agarose gels. The *lpxA* and *lpxH* genes from *N. meningitidis* strain H44/76 (21) were amplified by PCR and cloned into the broad host range expression vector pMMB67EH. PCR products and plasmids were purified using the Clean-Up System and Plasmid Extraction kit, respectively (both from Promega). Purified plasmid and PCR products were digested with restriction enzymes (Fermentas) whose sites were included in the primers (Table S2) and subsequently ligated together. To generate pMMB67EH-LpxH<sub>Nm</sub>-LpxA<sub>Nm</sub>, a PCR fragment containing *lpxH* was cloned into pMMB67EH-LpxA<sub>Nm</sub>. All plasmids were sequenced at Macrogen (Seoul, Korea). Plasmids were then used to transform *E. coli* strains BL21(DE3) and SM10 $\lambda$ pir for protein production and for subsequent transfer to *B. pertussis*, respectively. The transfer to *B. pertussis* was performed by conjugation using ampicillin and nalidixic acid for selection and counterselection, respectively.

### RNA extraction and RT-PCR

RNA was obtained from exponentially growing cultures as described previously (22). Pure RNA was used immediately to generate cDNA using the Transcriptor High Fidelity cDNA Synthesis Kit (Roche). RNA, cDNA, and genomic DNA were used as templates in PCRs with the primers listed in Table S2.

### SDS-PAGE and Western blotting

Bacteria from liquid cultures grown to an  $A_{600}$  of ~1 for *E. coli* or an  $A_{590}$  of ~0.5 for *B. pertussis* were collected by centrifugation, adjusted to an optical density of 5.0, mixed 1:1 with double-strength sample buffer, and heated for 10 min at 100 °C. Proteins were separated by SDS-PAGE on gels containing 14% acrylamide. After SDS-PAGE, proteins were transferred to nitrocellulose membranes and detected with anti-His<sub>6</sub> tag antibodies (Sigma-Aldrich) following procedures described previously (23).

### LPS purification and analysis

LPS was isolated from bacteria with hot phenol–water (24) and purified further by solid-phase extraction (SPE) on C8 reverse-phase cartridges. Briefly, bacteria were collected from cultures by centrifugation, suspended in water at 70 °C, and mixed with 0.8 volumes of phenol at the same temperature.

## Substrate specificity of *B. pertussis* LpxH

After separating the aqueous and phenolic phases by centrifugation, the aqueous phase was prepared for SPE by adding one volume of 0.356 M triethylammonium acetate (pH 7) (solvent A) and  $\frac{1}{3}$  volume of 2-propanol:water:triethylamine:acetic acid (70:30:0.03:0.01 (v/v)) (pH 8.9) (solvent B). LPS extracts were purified simultaneously by SPE on reverse-phase Sep-Pak C8 cartridges (3-ml syringe barrel-type Vac cartridge, 200 mg of C8 resin, Waters) using a 20-position vacuum manifold (Waters). Cartridges were conditioned for SPE by consecutively applying  $3 \times 1$  ml of solvent B, 2-propanol:water:triethylamine:acetic acid (10:90:0.03:0.01 (v/v)) (pH 8.9) (solvent C), 0.07 mM triethylammonium acetate (pH 7) (solvent D), and solvent A under a vacuum. Then samples were loaded into the cartridges, and each cartridge was washed with  $3 \times 1$  ml of solvents A, D, and C, in this order. LPS were eluted from the columns by applying  $2 \times 0.3$  ml of solvent B. Eluates were dried in a centrifugal vacuum concentrator and suspended in water. The purity and integrity of purified samples were judged by Tricine-SDS-PAGE combined with LPS silver and Coomassie staining. Negative-ion ESI Fourier transform (FT) MS of purified LPS was performed on an LTQ Orbitrap XL instrument (Thermo Scientific). LPS samples were dissolved in a mixture of 2-propanol, water, and triethylamine (50:50:0.001 (v/v/v)) (pH 8.5) and infused into the mass spectrometer by nano-ESI using gold-coated pulled glass capillaries (25). The spray voltage was set to from  $-1.3$  to  $-1.85$  kV, and the temperature of the heated capillary was  $250$  °C. Under these ionization conditions, no appreciable fragmentation of LPS was observed. To record lipid A mass spectra, nano-ESI-FT-MS of LPS was performed with in-source CID at a potential difference of 100 V. In-source CID under this setting produced intense fragment ions corresponding to intact lipid A domains, which originated from the rupture of the labile linkage between the nonreducing lipid A glucosamine and 3-deoxy-d-manno-oct-2-ulosonic acid. The lipid A compositions proposed are based on the chemical structure of the LPS from *B. pertussis* reported previously (26). Mass-to-charge ratios given refer to monoisotopic molecular masses.

Singly deprotonated lipid A ions generated by in-source CID of LPS from *B. pertussis* B213-pLpxH<sub>Nm</sub> and *B. pertussis* B213-pLpxH<sub>Nm</sub>-LpxA<sub>Nm</sub> were subjected to tandem MS by CID at a normalized collision energy of 35% on an LTQ Orbitrap XL Instrument (Thermo Scientific). Fourier Transform MS/MS lipid A mass spectra were recorded at a resolution of 60,000 at  $m/z$  400.

### Bioinformatic analysis

Multiple sequence alignment of the LpxH sequences was performed using the Clustal Omega web portal with default settings (27). Visualization and coloring of the alignment were performed using Jalview (28). Homology modeling of LpxH of *B. pertussis* was performed using Rosetta 3.8 (29, 30). Briefly, modeling was based on the structures of LpxH in complex with lipid X from *H. influenzae* (PDB code 5K8K) and *P. aeruginosa* (PDB codes 5B49, 5B4A, and 5B4B). Sets of 5000 models were built with either a 3OH-C10 or a 3OH-C14 chain on the 3 position of the ligand. For each of the sets, the best 1000 models by score were clustered using Calibur (31). Of those, the lowest-energy structures of the 10 largest clusters were combined into

an ensemble and refined using the Haddock refinement server (32). All final models were evaluated based on energy and cluster size. Visualization and image generation was done using the PyMOL Molecular Graphics System provided by SBGrid (33).

### TLR4 stimulation assays

Human NF- $\kappa$ B/SEAP reporter HEK293-Blue cells transfected with either human or mouse TLR4 in combination with MD-2 and CD14 (InvivoGen) were used in this study. Both cell lines contain an NF- $\kappa$ B-dependent secreted embryonic alkaline phosphatase (SEAP) reporter gene, which is expressed after TLR4 signaling. The cells were grown in HEK-Blue culture medium as described before (13) at  $37$  °C in a 5% saturated CO<sub>2</sub> atmosphere. For TLR4 activation, HEK-Blue cells ( $2.5 \times 10^4$ ) were incubated with serial dilutions of purified LPS in a 96-well plate. After 17 h of incubation at  $37$  °C, supernatants were collected and incubated with  $1$  mg ml<sup>-1</sup> of the SEAP substrate *para*-nitrophenyl phosphate in  $1$  M diethanolamine substrate buffer (pH 9.8), and the A<sub>405</sub> was measured using an ELISA reader. For each strain, the log response ratio was calculated as the log<sub>10</sub> of the ratio between sample and control (nonstimulated cells). Two-way analysis of variance (Dunnett's multiple comparison test) was used to analyze the data for statistical significance.

### Antibiotic sensitivity assays

The antibiotic susceptibility of *B. pertussis* was tested following methods described previously (34) with some modifications. Briefly, serial dilutions of antibiotics were prepared in PBS, and  $50$   $\mu$ l of each dilution was transferred to a 96-well microtiter plate (final antibiotic concentrations ranging from  $0.2$   $\mu$ g ml<sup>-1</sup> to  $2$  mg ml<sup>-1</sup>). *B. pertussis* strains were grown to log phase in Verwey medium (A<sub>590</sub> of 0.2–0.6). Bacterial suspensions were then diluted to a final A<sub>590</sub> of 0.2 in Verwey medium, and  $50$ - $\mu$ l aliquots were added to each well in the microtiter plate and incubated under static conditions for 1 h. No differences in the A<sub>590</sub> of the bacterial cultures were detected before and after incubation. Then,  $50$   $\mu$ l of each sample was diluted, and the number of surviving bacteria was determined by plating 10-fold serial dilutions onto BG plates. Antibiotic concentrations that resulted in a bacterial survival of  $\sim 20$ – $60\%$  and that showed reproducible results were selected ( $1$   $\mu$ g ml<sup>-1</sup> of rifampicin,  $2$  mg ml<sup>-1</sup> of vancomycin, and  $2$   $\mu$ g ml<sup>-1</sup> of chloramphenicol). For each strain, the number of colony-forming units was relative to the control (no antibiotic). For each experiment, at least three biological replicates were performed, and Student's *t* test was used to analyze the data for statistical significance.

*Author contributions*—J. A. and J. T. conceptualization; J. A. and J. T. data curation; J. A. software; J. A., E. P., and J. T. formal analysis; J. A., P. v. d. L., and J. T. supervision; J. A. validation; J. A., E. P., E. d. J., J. P.-O., and J. S. investigation; J. A., P. v. d. L., and J. T. visualization; J. A., E. P., and J. S. methodology; J. A. and J. T. writing-original draft; J. A., P. v. d. L., and J. T. project administration; J. A., E. d. J., J. P.-O., J. S., P. v. d. L., and J. T. writing-review and editing; P. v. d. L. and J. T. resources; P. v. d. L. and J. T. funding acquisition.

*Acknowledgments*—We thank Sandra Ochoa and Ria van Boxtel (Utrecht University) for assistance.

## References

- Raetz, C. R., and Whitfield, C. (2002) Lipopolysaccharide endotoxins. *Annu. Rev. Biochem.* **71**, 635–700 [CrossRef Medline](#)
- Needham, B. D., and Trent, M. S. (2013) Fortifying the barrier: the impact of lipid A remodelling on bacterial pathogenesis. *Nat. Rev. Microbiol.* **11**, 467–481 [CrossRef Medline](#)
- Raetz, C. R., Reynolds, C. M., Trent, M. S., and Bishop, R. E. (2007) Lipid A modification systems in gram-negative bacteria. *Annu. Rev. Biochem.* **76**, 295–329 [CrossRef Medline](#)
- Wyckoff, T. J., Lin, S., Cotter, R. J., Dotson, G. D., and Raetz, C. R. (1998) Hydrocarbon rulers in UDP-*N*-acetylglucosamine acyltransferases. *J. Biol. Chem.* **273**, 32369–32372 [CrossRef Medline](#)
- Smith, E. W., Zhang, X., Behzadi, C., Andrews, L. D., Cohen, F., and Chen, Y. (2015) Structures of *Pseudomonas aeruginosa* LpxA reveal the basis for its substrate selectivity. *Biochemistry* **54**, 5937–5948 [CrossRef Medline](#)
- Shah, N. R., Albitar-Nehme, S., Kim, E., Marr, N., Novikov, A., Caroff, M., and Fernandez, R. C. (2013) Minor modifications to the phosphate groups and the C3' acyl chain length of lipid A in two *Bordetella pertussis* strains, BP338 and 18–323, independently affect Toll-like receptor 4 protein activation. *J. Biol. Chem.* **288**, 11751–11760 [CrossRef Medline](#)
- Stöver, A. G., Da Silva Correia, J., Evans, J. T., Cluff, C. W., Elliott, M. W., Jeffery, E. W., Johnson, D. A., Lacy, M. J., Baldrige, J. R., Probst, P., Ulevitch, R. J., Persing, D. H., and Hershberg, R. M. (2004) Structure-activity relationship of synthetic toll-like receptor 4 agonists. *J. Biol. Chem.* **279**, 4440–4449 [CrossRef Medline](#)
- Steeghs, L., Berns, M., ten Hove, J., de Jong, A., Roholl, P., van Alphen, L., Tommassen, J., and van der Ley, P. (2002) Expression of foreign LpxA acyltransferases in *Neisseria meningitidis* results in modified lipid A with reduced toxicity and retained adjuvant activity. *Cell. Microbiol.* **4**, 599–611 [CrossRef Medline](#)
- Clark, T. A. (2014) Changing pertussis epidemiology: everything old is new again. *J. Infect. Dis.* **209**, 978–981 [CrossRef Medline](#)
- Sealey, K. L., Belcher, T., and Preston, A. (2016) *Bordetella pertussis* epidemiology and evolution in the light of pertussis resurgence. *Infect. Genet. Evol.* **40**, 136–143 [CrossRef Medline](#)
- Geurtsen, J., Steeghs, L., Hamstra, H. J., ten Hove, J., de Haan, A., Kuipers, B., Tommassen, J., and van der Ley, P. (2006) Expression of the lipopolysaccharide-modifying enzymes PagP and PagL modulates the endotoxic activity of *Bordetella pertussis*. *Infect. Immun.* **74**, 5574–5585 [CrossRef Medline](#)
- Caroff, M., Deprun, C., Richards, J. C., and Karibian, D. (1994) Structural characterization of the lipid A of *Bordetella pertussis* 1414 endotoxin. *J. Bacteriol.* **176**, 5156–5159 [CrossRef Medline](#)
- Sweet, C. R., Preston, A., Toland, E., Ramirez, S. M., Cotter, R. J., Maskell, D. J., and Raetz, C. R. (2002) Relaxed acyl chain specificity of *Bordetella* UDP-*N*-acetylglucosamine acyltransferases. *J. Biol. Chem.* **277**, 18281–18290 [CrossRef Medline](#)
- Brummelman, J., Veerman, R. E., Hamstra, H. J., Deuss, A. J., Schuijt, T. J., Sloots, A., Kuipers, B., van Els, C. A., van der Ley, P., Mooi, F. R., Han, W. G., and Pinelli, E. (2015) *Bordetella pertussis* naturally occurring isolates with altered lipooligosaccharide structure fail to fully mature human dendritic cells. *Infect. Immun.* **83**, 227–238 [CrossRef Medline](#)
- Richie, D. L., Takeoka, K. T., Bojkovic, J., Metzger, L. E., 4th, Rath, C. M., Sawyer, W. S., Wei, J. R., and Dean, C. R. (2016) Toxic accumulation of LPS pathway intermediates underlies the requirement of LpxH for growth of *Acinetobacter baumannii* ATCC 19606. *PLoS ONE* **11**, e0160918 [CrossRef Medline](#)
- Cho, J., Lee, C. J., Zhao, J., Young, H. E., and Zhou, P. (2016) Structure of the essential *Haemophilus influenzae* UDP-diacetylglucosamine pyrophosphohydrolase LpxH in lipid A biosynthesis. *Nat. Microbiol.* **1**, 16154 [CrossRef Medline](#)
- Okada, C., Wakabayashi, H., Kobayashi, M., Shinoda, A., Tanaka, I., and Yao, M. (2016) Crystal structures of the UDP-diacetylglucosamine pyrophosphohydrolase LpxH from *Pseudomonas aeruginosa*. *Sci. Rep.* **6**, 32822 [CrossRef Medline](#)
- Vadovic, P., Fodorová, M., and Toman, R. (2007) Structural features of lipid A of *Piscirickettsia salmonis*, the etiological agent of the salmonid rickettsial septicemia. *Acta Virol.* **51**, 249–259 [Medline](#)
- Li, Y., Powell, D. A., Shaffer, S. A., Rasko, D. A., Pelletier, M. R., Leszyk, J. D., Scott, A. J., Masoudi, A., Goodlett, D. R., Wang, X., Raetz, C. R., and Ernst, R. K. (2012) LPS remodeling is an evolved survival strategy for bacteria. *Proc. Natl. Acad. Sci. U.S.A.* **109**, 8716–8721 [CrossRef Medline](#)
- Verwey, W. F., Thiele, E. H., Sage, D. N., and Schuchardt, L. F. (1949) A simplified liquid culture medium for the growth of *Hemophilus pertussis*. *J. Bacteriol.* **58**, 127–134 [Medline](#)
- Piet, J. R., Huis in 't Veld, R. A., van Schaik, B. D., van Kampen, A. H., Baas, F., van de Beek, D., Pannekoek, Y., and van der Ende, A. (2011) Genome sequence of *Neisseria meningitidis* serogroup B strain H44/76. *J. Bacteriol.* **193**, 2371–2372 [CrossRef Medline](#)
- Arenas, J., Paganelli, F. L., Rodríguez-Castaño, P., Cano-Crespo, S., van der Ende, A., van Putten, J. P., and Tommassen, J. (2016) Expression of the gene for autotransporter AutB of *Neisseria meningitidis* affects biofilm formation and epithelial transmigration. *Front. Cell. Infect. Microbiol.* **6**, 162 [Medline](#)
- Arenas, J., de Maat, V., Catón, L., Kjekshus, M., Herrero, J. C., Ferrara, F., and Tommassen, J. (2015) Fratricide activity of MafB protein of *N. meningitidis* strain B16B6. *BMC Microbiol.* **15**, 156 [CrossRef Medline](#)
- Westphal, O., and Jann, K. (1965) Bacterial lipopolysaccharide extraction with phenol-water and further applications of the procedure. *Meth. Carbohydrates Chem.* **5**, 83–91
- Kondakov, A., and Lindner, B. (2005) Structural characterization of complex bacterial glycolipids by Fourier transform mass spectrometry. *Eur. J. Mass Spectrom. (Chichester)* **11**, 535–546 [CrossRef Medline](#)
- Caroff, M., Brisson, J., Martin, A., and Karibian, D. (2000) Structure of the *Bordetella pertussis* 1414 endotoxin. *FEBS Lett.* **477**, 8–14 [CrossRef Medline](#)
- Sievers, F., Wilm, A., Dineen, D., Gibson, T. J., Karplus, K., Li, W., Lopez, R., McWilliam, H., Remmert, M., Söding, J., Thompson, J. D., and Higgins, D. G. (2011) Fast, scalable generation of high-quality protein multiple sequence alignments using Clustal Omega. *Mol. Syst. Biol.* **7**, 539 [CrossRef Medline](#)
- Waterhouse, A. M., Procter, J. B., Martin, D. M., Clamp, M., and Barton, G. J. (2009) Jalview version 2: a multiple sequence alignment editor and analysis workbench. *Bioinformatics* **25**, 1189–1191 [CrossRef Medline](#)
- Song, Y., DiMaio, F., Wang, R. Y., Kim, D., Miles, C., Brunette, T., Thompson, J., and Baker, D. (2013) High-resolution comparative modeling with RosettaCM. *Structure* **21**, 1735–1742 [CrossRef Medline](#)
- Leaver-Fay, A., Tyka, M., Lewis, S. M., Lange, O. F., Thompson, J., Jacak, R., Kaufman, K., Renfrew, P. D., Smith, C. A., Sheffler, W., Davis, I. W., Cooper, S., Treuille, A., Mandell, D. J., Richter, F., et al. (2011) ROSETTA3: an object-oriented software suite for the simulation and design of macromolecules. *Methods Enzymol.* **487**, 545–574 [CrossRef Medline](#)
- Li, S. C., and Ng, Y. K. (2010) Calibur: a tool for clustering large numbers of protein decoys. *BMC Bioinformatics* **11**, 25 [CrossRef Medline](#)
- van Zundert, G. C. P., Rodrigues, J. P. G. L. M., Trellet, M., Schmitz, C., Kastrius, P. L., Karaca, E., Melquiond, A. S. J., van Dijk, M., de Vries, S. J., and Bonvin, A. M. J. J. (2016) The HADDOCK2.2 webserver: user-friendly integrative modeling of biomolecular complexes. *J. Mol. Biol.* **428**, 720–725 [CrossRef Medline](#)
- Morin, A., Eisenbraun, B., Key, J., Sanschagrin, P. C., Timony, M. A., Ottaviano, M., and Sliz, P. (2013) Collaboration gets the most out of software. *eLife* **2**, e01456 [CrossRef Medline](#)
- Shah, N. R., Hancock, R. E., and Fernandez, R. C. (2014) *Bordetella pertussis* lipid: a glucosamine modification confers resistance to cationic antimicrobial peptides and increases resistance to outer membrane perturbation. *Antimicrob. Agents Chemother.* **58**, 4931–4934 [CrossRef Medline](#)